

An Isolated Limb Infusion Method Allows for Broad Distribution of rAAVrh74.MCK.GALGT2 to Leg Skeletal Muscles in the Rhesus Macaque

Rui Xu,¹ Ying Jia,¹ Deborah A. Zygmunt,¹ Megan L. Cramer,^{1,2} Kelly E. Crowe,^{1,2} Guohong Shao,¹ Agatha E. Maki,¹ Haley N. Guggenheim,¹ Benjamin C. Hood,¹ Danielle A. Griffin,¹ Ellyn Peterson,¹ Brad Bolon,³ John P. Cheatham,⁴ Sharon L. Cheatham,⁴ Kevin M. Flanigan,^{1,4} Louise R. Rodino-Klapac,^{1,4} Louis G. Chicoine,^{1,4} and Paul T. Martin^{1,4}

¹Center for Gene Therapy, The Research Institute at Nationwide Children's Hospital, 700 Children's Drive, Columbus, OH 43205, USA; ²Graduate Program in Molecular, Cellular and Developmental Biology, The Ohio State University, Columbus, OH 43210, USA; ³GEMPath Inc., Longmont, CO 80504, USA; ⁴Department of Pediatrics, The Ohio State University College of Medicine, Columbus, OH 43210, USA

Recombinant adeno-associated virus (rAAV)rh74.MCK.GALGT2 is a muscle-specific gene therapy that is being developed to treat forms of muscular dystrophy. Here we report on an isolated limb infusion technique in a non-human primate model, where hindlimb blood flow is transiently isolated using balloon catheters to concentrate vector in targeted leg muscles. A bilateral dose of 2.5×10^{13} vector genomes (vg)/kg/limb was sufficient to induce GALGT2-induced glycosylation in 10%–60% of skeletal myofibers in all leg muscles examined. There was a 19-fold \pm 6-fold average limb-wide increase in vector genomes per microgram genomic DNA at a bilateral dose of 2.5×10^{13} vg/kg/limb compared with a bilateral dose of 6×10^{12} vg/kg/limb. A unilateral dose of 6×10^{13} vg/kg/limb showed a 12- \pm 3-fold increase in treated limb muscles compared to contralateral untreated limb muscles, which received vector only after release into the systemic circulation from the treated limb. Variability in AAV biodistribution between different segments of the same muscle was 125% \pm 18% for any given dose, while variability between the same muscle for any given treatment dose was 45% \pm 7%. These experiments demonstrate that treatment of muscles throughout the leg with rAAVrh74.MCK.GALGT2 can be accomplished safely using an isolated limb infusion technique, where balloon catheters transiently isolate the limb vasculature, but that intra- and inter-muscle transduction variability is a significant issue.

INTRODUCTION

Recombinant adeno-associated virus (rAAV) is increasingly being utilized as a vector delivery method for therapeutic transgenes. There are, however, significant obstacles to systemic delivery of AAV, including cost of manufacturing, effectiveness of tissue transduction, vector-induced immunity, and tissue toxicity.^{1–5} Systemic AAV delivery as a therapy is a particular challenge for the treatment of skeletal muscles, which comprise 35%–45% of human body mass in young adults and 30%–40% of body mass in aged adults.⁶ In diseases such as Duchenne muscular dystrophy (DMD), an ideal treatment

would treat all muscles throughout the body plan. Otherwise, muscle mass is lost over time, leading to generalized weakness and loss of ambulation.^{7,8} Here we have studied an isolated whole limb infusion method with the aim of providing a method to treat all leg muscles at doses lower than those typically required with systemic intravenous (i.v.) delivery.

The vector we have used for this study, rAAVrh74.MCK.GALGT2, allows for vascular delivery of AAV to muscle, and it utilizes a muscle-specific creatine kinase (MCK) promoter to overexpress the human GALGT2 cDNA (also called *B4GALNT2*) specifically in cardiac and skeletal muscle cells.^{9,10} GALGT2 overexpression in muscle cells can inhibit muscular dystrophy in mouse models of DMD, congenital muscular dystrophy 1A (MDC1A), and limb girdle muscular dystrophy 2D and 2I (LGMD2D and LGMD2I).^{9,11–14} It does so, in part, by stabilizing the muscle membrane to protect it from eccentric contraction-induced injury and by inducing the overexpression of surrogate proteins known to inhibit (or impact) muscular dystrophy, including utrophin, plectin1, agrin, laminin $\alpha 4$, and laminin $\alpha 5$.^{11–13,15–23} GALGT2 can be a remarkably potent surrogate gene therapy; GALGT2 overexpression is required in only 15%–20% of mdx myofibers in the extensor digitorum longus (EDL) muscle to achieve significant increases in specific force and prevention of force drop during eccentric contractions.²³

Significant progress has been made in targeted vascular limb delivery using AAV. Early rodent studies often used high delivery volumes and agents such as histamine or papaverine to increase vasodilation and capillary leakage to allow viral or DNA entry into muscles.^{24–26} More recent studies, however, of rodents, dogs, and macaques have

Received 4 January 2018; accepted 5 June 2018;
<https://doi.org/10.1016/j.omtm.2018.06.002>

Correspondence: Paul T. Martin, Center for Gene Therapy, The Research Institute at Nationwide Children's Hospital, 700 Children's Drive, Columbus, OH 43205, USA.

E-mail: paul.martin@nationwidechildrens.org



Table 1. Study Design for ILI

Subject	Age (Years)	Gender	Weight (kg)	Limb Treated	Study Agent	Dose (vg/kg)	ILI Mode of Delivery	Endpoint
RQ8761	6.69	Male	11.5	left	rAAVrh74.MCK.GALGT2	6.00E+12	bilateral	3 months
				right	rAAVrh74.MCK.GALGT2	6.00E+12		
07D147	9.15	male	8.92	left	rAAVrh74.MCK.GALGT2	2.50E+13	bilateral	3 months
				right	rAAVrh74.MCK.GALGT2	2.50E+13		
04C034	12.25	female	7.93	left	–	0	unilateral	3 months
				right	rAAVrh74.MCK.GALGT2	6.00E+13		

achieved success using methods where vasodilators were not required and where smaller loading volumes were used. These include studies of Factor IX overexpression in the limb muscles of Factor IX-deficient dogs, where prolonged functional improvement in bleeding time could be achieved after limb infusion; studies in mdx mice, where both micro-dystrophin and *GALGT2* transgene overexpression could improve specific force and decrease force drop during eccentric contraction-induced injury after isolated femoral artery delivery to the limb; studies in Golden Retriever muscular dystrophy (GRMD) dogs, where U7-driven dystrophin gene exon skipping oligonucleotides or micro-dystrophin gene therapy could induce dystrophin protein expression and improve limb muscle function; and rhesus macaques, where targeted AAV delivery via the sural artery showed widespread transduction of the gastrocnemius muscle after vascular delivery of *GALGT2* and micro-dystrophin.^{10,23,27–34}

Partial limb exsanguination shows additional benefits in studies of alkaline phosphatase transgene delivery in the macaque.³¹ High-pressure volume loading via i.v. delivery has also shown promise for isolated limb treatment in dystrophic dogs and humans.^{29,35} While use of vascular clamps or tourniquets has allowed for effective regional delivery to limbs in a number of experiments using large animal models, we wished to expand upon these studies to integrate the use of balloon catheters to isolate both the venous and arterial limb blood flow. Balloon catheters are commonly used in clinical medicine for a variety of techniques, including isolation of blood flow, blood clot removal, and focal drug delivery to the heart and other organs. We sought to apply this technique to bilateral limb delivery in the leg muscles, as only bilateral delivery will allow for full protection against loss of ambulation.

RESULTS

Delivery of rAAVrh74.MCK.GALGT2 by Isolated Limb Infusion Allows for Broad Expression of *GALGT2* in Leg Skeletal Muscles

In our previous studies in the rhesus macaque where we targeted rAAVrh74.MCK.GALGT2 to a single limb muscle, the gastrocnemius, using isolated vascular infusion, we found that a dose of 2×10^{12} vector genomes (vg)/kg was sufficient to transduce the majority of both the medial and lateral heads of the muscle with *GALGT2*.¹⁰ Here our goal was to expand this method to treat all of the muscles of the leg. To do this, we increased the dose 3- (6×10^{12} vg/kg), 12.5- (2.5×10^{13} vg/kg), or 30-fold (6×10^{13} vg/kg) from the amount

previously used. Only macaques that were sero-negative for total anti-rAAVrh74 capsid antibodies were used. In addition, macaques were screened for expression of *Mamu* (major histocompatibility complex [MHC] class I) haplotypes to ensure they did not express the *Mamu-0A0201* allele, which we had previously shown could allow for the presentation of a human *GALGT2* peptide that differed from the macaque sequence in a way that stimulated a CD8+ cytotoxic T cell response in vector-treated muscles.¹⁰

In each experiment, balloon catheters were inserted into the femoral artery and femoral vein, moved distally to the pelvic region, and inflated in order to isolate the limb vasculature for 12 min. A 2-mL/kg flush of lactated Ringer's (LR) solution was given over 1 min, after which rAAVrh74.MCK.GALGT2 was delivered distally through a side port in the catheter in 8 mL/kg LR over 1 min. Vector was allowed to remain in the isolated limb for a total of 10 min, after which a second 2-mL/kg flush of LR was given over 1 min. The catheter balloons were then deflated to remove vascular occlusion and allow vector to enter the general blood flow. Catheters were then removed and a hemepatch was applied to stop bleeding.

Three experiments were done, each using one rhesus macaque (Table 1). In the first experiment (subject RQ8761), both legs were treated (bilateral treatment) with 6×10^{12} vg/kg rAAVrh74.MCK.GALGT2, for a total dose of 1.2×10^{13} vg/kg. In the second experiment (subject 07D147), both legs were treated (bilateral treatment) with 2.5×10^{13} vg/kg, for a total dose of 5×10^{13} vg/kg. In the third experiment (subject 04C034), a single limb was treated (unilateral treatment) with 6×10^{13} vg/kg rAAVrh74.MCK.GALGT2, for a total dose of 6×10^{13} vg/kg. The contralateral limb in subject 04C034 underwent vascular access and catheters were inserted, but balloons were not inflated and no vector was given: this contralateral limb, therefore, received vector only after it was released from the treated limb into the systemic circulation. In all three experiments, vector was diluted with LR for delivery.

At 3 months after treatment, animals were necropsied and 14 different leg muscles (vastus lateralis, vastus medialis, vastus intermedius, semimembranosus, semitendinosus, sartorius, gracilis, biceps femoris, rectus femoris, tibialis anterior, extensor digitorum longus, soleus, medial gastrocnemius, and lateral gastrocnemius) were dissected. Between 5 and 16 muscle blocks, each with rostral-caudal

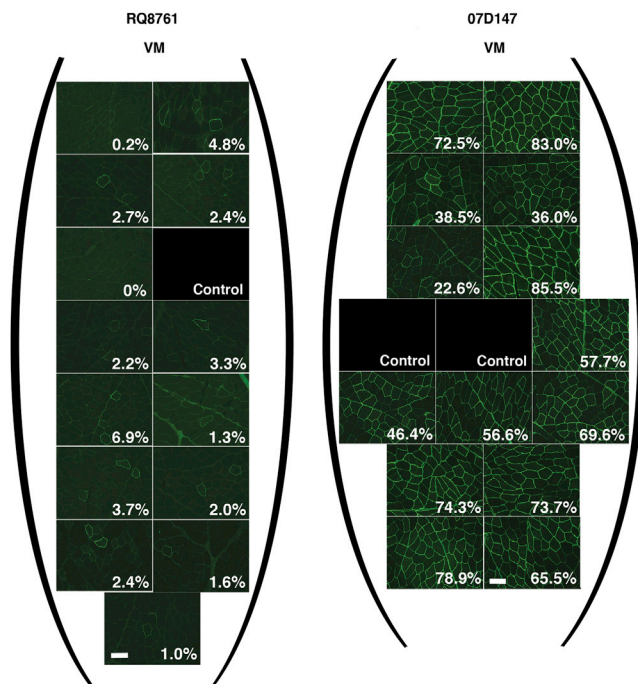


Figure 1. Heatmap of GALGT2-Induced Cytotoxic T Cell Glycan Overexpression in the Vastus Medialis Muscle after Bilateral Isolated Limb Infusion with rAAVrh74.MCK.GALGT2

A dose of 6×10^{12} vg/kg (left, RQ8761) or 2.5×10^{13} vg/kg (right, 07D147) rAAVrh74.MCK.GALGT2 was given by the isolated limb infusion method, and 15–16 blocks from the vastus medialis (VM) muscle were dissected, snap-frozen, cut in cross-section, and stained with *Wisteria floribunda* agglutinin (WFA) to identify GALGT2-induced glycosylation at 3 months post-treatment. Percentages of GALGT2-expressing myofibers were quantified as described in the [Materials and Methods](#). Control shows no primary stain (no WFA). Scale bars, 100 μ m.

and medial-lateral positions marked, were taken from each muscle in order to generate a heatmap of cytotoxic T cell glycan overexpression (resulting from overexpression of GALGT2). The three muscles immediately outside the vascular isolation zone of the leg (gluteus minimus, gluteus medius, and gluteus maximus) were also analyzed, as were muscles further removed, including diaphragm, triceps brachii, biceps brachii, and heart. Non-muscle organs, including liver, lung, kidney, spleen, gonads, stomach, pancreas, urinary bladder, brain, popliteal and mesenteric lymph nodes, and sural and femoral arteries, were also dissected, and single blocks were taken to understand biodistribution after vector release into the systemic circulation.

GALGT2-induced glycosylation of the muscle with the cytotoxic T cell glycan was assayed using *Wisteria floribunda* agglutinin (WFA) staining, while copies of AAV vector genomes was measured by qPCR, both as before.¹⁰ We found that a bilateral dose of 2.5×10^{13} vg/kg/limb (subject 07D147) was superior to a bilateral dose of 6×10^{12} vg/kg/limb (subject RQ8761). This was most apparent in the vastus medialis (VM) segment of the quadriceps muscle (Figure 1). The average percentage of myofibers overexpressing GALGT2 was $61\% \pm 5\%$ among 14 VM segments analyzed within one

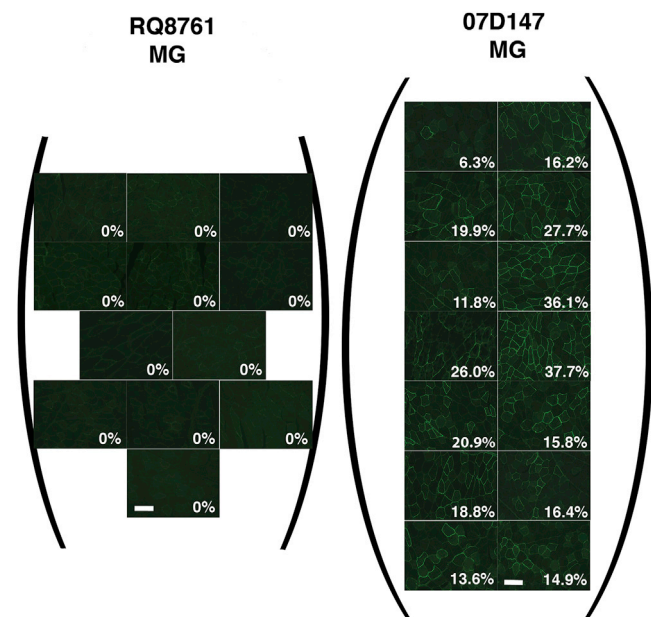


Figure 2. Heatmap of GALGT2-Induced Cytotoxic T Cell Glycan Overexpression in the Medial Gastrocnemius Muscle after Bilateral Isolated Limb Infusion with rAAVrh74.MCK.GALGT2

A dose of 6×10^{12} vg/kg (left, RQ8761) or 2.5×10^{13} vg/kg (right, 07D147) rAAVrh74.MCK.GALGT2 was given by the isolated limb infusion method, and 15–16 blocks from the medial gastrocnemius (MG) muscle were dissected, snap-frozen, cut in cross-section, and stained with *Wisteria floribunda* agglutinin (WFA) to identify GALGT2-induced glycosylation at 3 months post-treatment. Percentages of GALGT2-expressing myofibers were quantified as described in the [Materials and Methods](#). Scale bars, 100 μ m.

treated limb (with a range of 23%–85%) using a dose of 2.5×10^{13} vg/kg/limb, compared to $3\% \pm 1\%$ in the VM at a dose of 6×10^{12} vg/kg/limb (with a range of 0%–7%, $p < 0.001$). Large staining differences between these two doses were also seen in muscles of the lower limb, including the medial gastrocnemius (Figure 2). The 2.5×10^{13} vg/kg/limb bilateral dose showed increased average GALGT2 overexpression in all 14 limb muscles relative to the 6×10^{12} vg/kg/limb bilateral dose (Figure 3A). This was also true when comparing the block with highest GALGT2-induced cytotoxic T cell glycan expression in each muscle (Figure 3B).

There was high variability in GALGT2 expression, both between muscles and between blocks within single muscles. This seemed most evident when comparing the medial to lateral positioning of the muscles in the upper leg relative to the medial positioning of the catheters. For example, within the three segments of the quadriceps of subject 07D147, the vastus medialis had the highest cytotoxic T cell glycan expression ($61\% \pm 5\%$), while the vastus lateralis had lower expression ($15\% \pm 5\%$) (Figure 3A). Likewise, the biceps femoris and rectus femoris showed lower cytotoxic T cell glycan expression than did muscles that had a more medial positioning, such as the sartorius and semimebranosus (Figure 3A). In all leg muscles below the knee (i.e., medial and lateral gastrocnemius, tibialis anterior, extensor

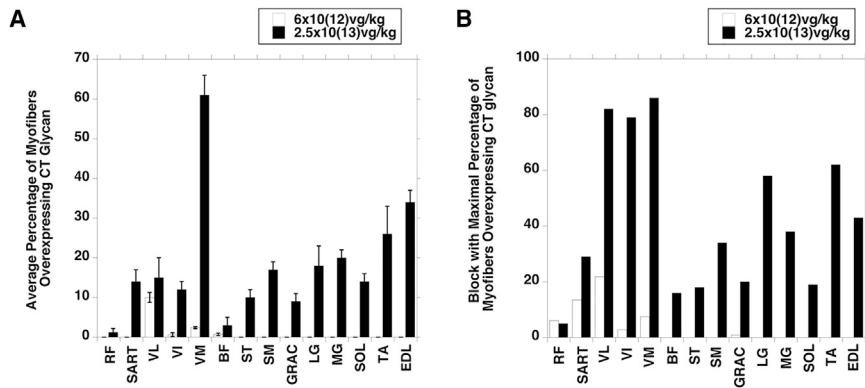


Figure 3. Comparison of GALGT2-Induced Glycan Overexpression in Leg Muscles after Bilateral Isolated Limb Infusion with rAAVrh74.MCK.GALGT2 (A and B) The average percentage of myofibers with GALGT2-induced glycan overexpression (A) and the block from each of 14 leg muscles with the highest level of expression (B) are shown for doses of 6×10^{12} vg/kg and 2.5×10^{13} vg/kg rAAVrh74.MCK.GALGT2 delivered using the isolated limb infusion method. Errors bars in A are SEM for $n = 6-16$ measures per muscle. CT, cytotoxic T cell. The muscles analyzed are as follows: RF, rectus femoris; SART, sartorius; VL, vastus lateralis; VI, vastus intermedius; VM, vastus medialis; BF, biceps femoris; ST, semitendinosus; SM, semimembranosus; GRAC, gracilis; LG, lateral gastrocnemius; MG, medial gastrocnemius; SOL, soleus; TA, tibialis anterior; and EDL, extensor digitorum longus.

digitorum longus, and soleus), however, the medial-lateral positioning did not appear to affect GALGT2 expression levels. For example, the right lateral gastrocnemius in subject 07D147 showed an average percent expression of $18\% \pm 4\%$ in 16 blocks analyzed, while the right medial gastrocnemius showed an average percent expression of $20\% \pm 2\%$ (Figure 3A). For subject 07D147, the average cytotoxic T cell glycan expression for all muscles above the knee was not significantly different than the average for all muscles below the knee ($17\% \pm 6\%$ above versus $22\% \pm 3\%$ below).

In general, at least some muscle segments within each of the 14 limb muscles showed significant GALGT2-induced cytotoxic T cell glycan overexpression (Figure 3B) when given 2.5×10^{13} vg/kg/limb, but there were a number of muscle segments that had no measurable cytotoxic T cell glycan overexpression. The failure rate of infusion (i.e., muscle blocks with no detectable cytotoxic T cell glycan overexpression) was higher for limb muscles above the knee than it was for muscles below the knee. For example, the failure rate of expression was at or above 50% for the rectus femoris (5 of 8 samples), biceps femoris (4 of 8), and vastus intermedius (6 of 12); was at an intermediate range for the semitendinosus (3 of 8), semimembranosus (2 of 12), and vastus lateralis (1 of 14); and was not present in the vastus medialis, sartorius, gracilis, medial gastrocnemius, lateral gastrocnemius, tibialis anterior, soleus, and extensor digitorum longus. Thus, some segments of muscles within the upper leg showed a lack of transduction even though the whole muscle, on average, showed significant levels of expression.

As some versions of the MCK promoter, for example, CK1 and CK6, preferentially express transgenes in fast (type 2B and 2X) muscle fiber types compared to slow (type 1 and 2A) muscle fiber types, we assessed in subject 07D147 the relative numbers of type 1, 2A, 2X, and 2B fibers with GALGT2-dependent glycosylation using sections of the vastus medialis, which contains significant numbers of fast fiber types, and the soleus, which is predominantly composed of slow muscle fiber types (Figure 4).³⁶ We found no alterations in the percentage of GALGT2-transduced fibers for any fiber type relative to predicted transduction level (calculated by multiplying the overall

percentage of GALGT2-overexpressing fibers in the section by the percentage of the particular fiber type in the same section). In this regard, it is important to point out that the MCK promoter used in rAAVrh74.MCK.GALGT2 contains promoter and enhancer elements that are identical to CK6, but it contains an additional 49 bp of gene sequence from exon 1, a non-coding exon, beginning at the transcription start site, which is present in CK7 (Figure S1). The CK7 version of the MCK promoter was shown to elevate expression in skeletal myoblasts 2-fold and in cardiomyocytes 5-fold relative to CK6.³⁶ Further, the CK7 version of the MCK promoter increases transduction of type 1 and 2A fibers relative to CK1 and CK6, making fiber type distribution of transgene expression more equivalent between fast and slow fibers, much as we have seen here.³⁶ It is also important to note, however, that, while the MCK promoter we have used shares the same the exon 1 sequence as CK7, it does not contain a mutated transcription start site that places a consensus initiator sequence in CK7, nor does it have the 63-bp deletion within the MCK promoter region present in CK7.³⁶ While these two additional modifications may further increase promoter potency in muscle, they may also reduce the specificity of muscle gene expression, and so they were not used here.

Muscles outside the treatment zone also showed some cytotoxic T cell glycan overexpression, demonstrating that vector released into the systemic circulation after isolated limb infusion (ILI) was able to transduce some muscles at a distance from the targeted limb. For the gluteus muscles, which were immediately outside the ILI vascular isolation zone, modest GALGT2-induced glycosylation was found, with $6\% \pm 3\%$ of myofibers transduced in the gluteus minimus and $4\% \pm 2\%$ of myofibers transduced in the gluteus maximus (with a range of 0%–18% per block) in subject 07D147. By contrast, no measurable glycosylation was seen in arm muscles (biceps or triceps, data not shown), which were further removed from the site of vascular isolation.

While there may be some instances where limb isolation would be needed to also prevent transduction of heart muscle, DMD certainly is not one such disease, as children with DMD often perish from heart

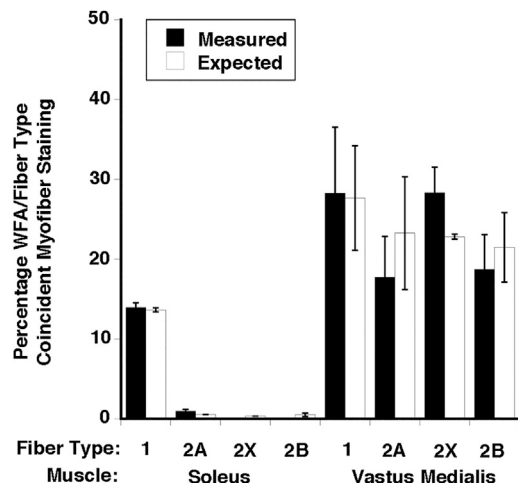


Figure 4. Distribution of WFA Staining among Muscle Fiber Types after Bilateral Isolated Limb Infusion with rAAVrh74.MCK.GALGT2

Muscle blocks of soleus and vastus medialis muscle from subject 07D147 were stained with WFA, to identify GALGT2-induced cytotoxic T cell glycan overexpression, and with antibodies specific to type 1, 2A, 2X, or 2B skeletal muscle fibers. The overall percentage of muscle fibers transduced with GALGT2 (WFA positive) was multiplied by the percentage of each myofiber type stained to generate expected coincidence values, and these were compared to measured coincidence values. Errors are SD for n = 2 muscle blocks per condition, with 5 measures per muscle block.

complications related to progressive cardiomyopathy.³⁷ As such, we undertook an analysis of WFA staining in heart muscle sections of subjects RQ8761 and 07D147 (Figures 5A and 5B). In subject RQ8761, we found very little WFA staining; however, a subset of intercalated disks, 11% ± 5%, were stained and identified by co-staining for N-cadherin. N-cadherin is a marker for intercalated disks, the cell-cell adhesive contacts that form between the ends of

cardiomyocytes.³⁸ In subject 07D147, which received a higher rAAVrh74.MCK.GALGT2 dose than subject RQ8761, we found a far more robust pattern of intercalated disk staining by WFA; fully 67% ± 14% of all N-cadherin-stained intercalated disks were scored positive for WFA co-staining. Thus, while strong AAV-mediated GALGT2 overexpression leads to glycosylation of the entire cardiomyocyte membrane in mice (data not shown), the presumably lower levels of GALGT2 gene expression that occurred here in treated macaque hearts nevertheless induced concentrations of βGalNAc at intercalated disk membranes in cardiomyocytes. While the function of such glycosylation is yet to be understood, deletion of *Galgt2* in mice, which eliminates the modest subcellular disk-like cytotoxic T cell glycan staining that occurs in the mouse heart, does induce negative changes in heart hemodynamic function.³⁹

We next measured biodistribution of AAV vector genomes in muscle blocks from the 14 treated limb muscles of each of the two legs treated at a bilateral dose of either 6×10^{12} vg/kg/limb (subject RQ8761) or 2.5×10^{13} vg/kg/limb (subject 07D147) (Figure 6A). In addition, here we added a third experiment in which we performed ILI on only one leg with a unilateral dose of 6×10^{13} vg/kg (subject 04C034) (Figure 6B). Subject 04C034 was basically treated with the same systemic dose as subject 07D147, only the dose was given unilaterally as opposed to bilaterally. The use of a unilateral dose in subject 04C034 also gave us the opportunity to measure vector uptake in the contralateral limb after it was released into the systemic circulation.

For the dose of 6×10^{12} vg/kg/limb, the average vector genomes per microgram (vg/μg) of genomic DNA in the two treated limbs ranged from 254 ± 21 vg/μg in the semitendinosus to $1.9 \pm 0.2 \times 10^4$ vg/μg in the gracilis. Biodistribution of vector genomes in two treated legs with 2.5×10^{13} vg/kg/limb ranged from $3,320 \pm 1,200$ vg/μg in the biceps femoris to $2.1 \pm 0.6 \times 10^5$ vg/μg in the sartorius (Figure 6A). The

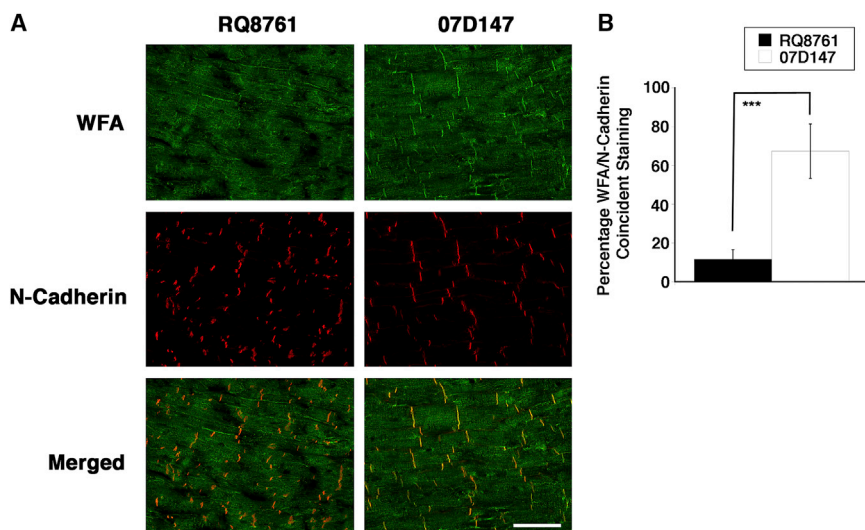


Figure 5. GALGT2-Induced Cytotoxic T Cell Glycan Staining of Intercalated Disks in Macaque Heart after Isolated Limb Infusion with rAAVrh74.MCK.GALGT2

(A) Heart sections from subject 07D147, given a total dose of 5×10^{13} vg/kg rAAVrh74.MCK.GALGT2, and subject RQ8761, given a total dose of 1.2×10^{13} vg/kg rAAVrh74.MCK.GALGT2, were stained with WFA (green), to identify GALGT2-induced glycosylation, and with antibody to N-cadherin (red), to identify intercalated disks. Scale bar, 100 μm. (B) Coincidence of WFA and N-cadherin staining at intercalated disks was quantified in heart sections from subject RQ8761 and 07D147. Errors are SD for n = 2–6 blocks per group. ***p < 0.001.

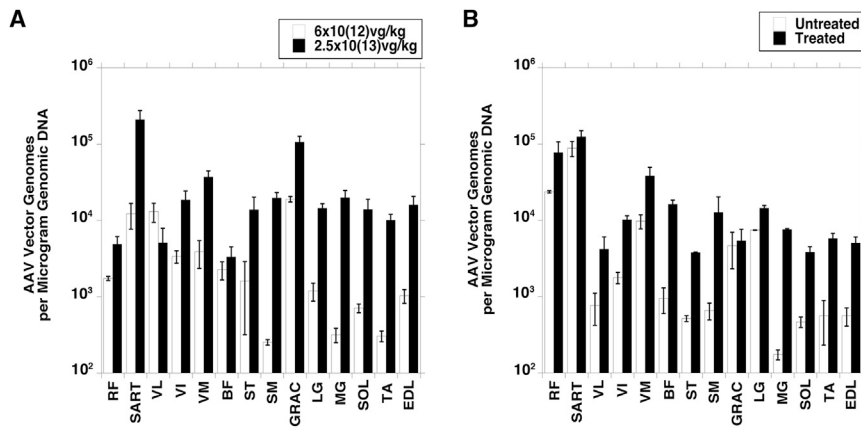


Figure 6. Comparison of rAAV Vector Genome Biodistribution after Vascular Delivery of rAAVrh74.MCK.GALGT2 Using Isolated Limb Infusion

(A) Average rAAV vector genomes (vg) per microgram of genomic DNA are compared for bilateral doses of 6×10^{12} vg/kg/limb and 2.5×10^{13} vg/kg/limb rAAVrh74.MCK.GALGT2 delivered by isolated limb infusion. (B) A unilateral dose of 6×10^{13} vg/kg/limb (treated) was compared to distribution in the contralateral limb (untreated). All measures were taken at 3 months post-treatment. Errors are SEM for $n = 6-16$ blocks per muscle. The muscles analyzed are as follows: RF, rectus femoris; SART, sartorius; VL, vastus lateralis; VI, vastus intermedius; VM, vastus medialis; BF, Biceps femoris; ST, semitendinosus; SM, semimembranosus; GRAC, gracilis; LG, lateral gastrocnemius; MG, medial gastrocnemius; SOL, soleus; TA, tibialis anterior; and EDL, extensor digitorum longus.

average increase in vector genomes per microgram genomic DNA in the 14 limb muscles at the 2.5×10^{13} vg/kg/limb dose was 19 ± 6 times what was seen at the 6×10^{12} vg/kg dose ($p < 0.03$; $n = 28$ muscles per group comparing 162 and 153 muscle blocks, respectively). The average variability (SD/mean) between different segments within the same muscle was almost identical for the 6×10^{12} vg/kg/limb and 2.5×10^{13} vg/kg/limb dose ($125\% \pm 22\%$ versus $126\% \pm 14\%$, respectively), as was the variability between the two treated muscles for each given bilateral dose ($49\% \pm 7\%$ versus $41\% \pm 6\%$). For the single limb treated unilaterally with 6×10^{13} vg/kg, there was a 12 ± 3 -fold increase in the 14 treated limb muscles compared with the same muscles in the contralateral limb, which received no treatment but was exposed to vector after it was released into the systemic circulation from the treated limb. The sartorius was the most transduced muscle in the untreated limb of subject 04C034 (Figure 6B). Heatmaps comparing single limb muscles in the upper leg (e.g., vastus medialis; Figure 7) showed uniformly higher AAV biodistribution among blocks taken from the macaque treated with 2.5×10^{13} vg/kg/limb dose compared to 6×10^{12} vg/kg/limb. There was, however, considerable block-to-block variability within each muscle. Biodistribution in subject 04C034 also showed uniformly higher levels in the treated limb than in the untreated limb (e.g., medial gastrocnemius; Figure 8).

Organ AAV Biodistribution

For both subjects 07D147 and 04C034, which received systemic doses of 5×10^{13} vg/kg and 6×10^{13} vg/kg, respectively, we analyzed AAV biodistribution in organs outside the infused limbs (Figure 9). As in many previous studies, the liver was the most highly transduced non-muscle organ, with $1-5 \times 10^6$ vg/ μ g, while levels in lung and spleen were also high ($1-5 \times 10^5$ vg/ μ g). The femoral artery and the inguinal lymph node also showed high expression (between 4×10^4 and 5×10^5 vg/ μ g). Kidney and pancreas showed lower levels of transduction (as high as 2×10^4 vg/ μ g), while heart, stomach, diaphragm, arm muscles (biceps brachii and triceps brachii), brain, urinary bladder, and gonads all showed low levels of transduction

(10^3 vg/ μ g or below). Subject 07D147 had 3.1×10^3 vg/ μ g in the heart, while subject RQ8761, which received the lower bilateral dose, had 1.7×10^2 vg/ μ g in the heart. The femoral artery, which received concentrated application of the vector during ILI, showed higher levels of transduction than did the sural artery, which was more distal to the infusion site. Likewise, the inguinal lymph node in the groin region, which drains the leg, showed higher levels of transduction than did the mesenteric lymph nodes in the abdomen.

T Cell Responses and AAV Antibodies

We assayed acquired T cell responses to both the AAV capsid and the GALGT2 transgenic protein (Table 2), much as was done previously.¹⁰ Peripheral blood mononuclear cells (PBMCs), which include T cells, were reacted with one of three overlapping peptide pools to the rAAVrh74 capsid protein or with one of two overlapping peptide pools to the human GALGT2 protein. These peptide pools collectively represent peptides encompassing the entire protein-coding sequence. Cells were then assayed by ELISpot assay for the induction of interferon- γ expression. Concanavalin A (ConA) was added as a positive control, with greater than 900 spots per 10^6 PBMCs in all conditions, and vehicle alone (0.25% DMSO) was added as a negative control, with less than 40 spots per condition (and almost always 0). Blood was assayed prior to treatment (baseline) and at 1, 2, and 3 months post-rAAVrh74.MCK.GALGT2 treatment. A measure of greater than 50 spots per 10^6 PBMCs was considered positive. Neither of the two macaque subjects given the highest dose of rAAVrh74.MCK.GALGT2 (07D147 and 04C034) showed positive T cell responses at 1, 2, or 3 months after treatment to any of the AAV capsid or GALGT2 peptide pools. We also assayed serum antibodies to rAAVrh74 capsid in the same two macaque subjects at the same time points (Table 3). Both subjects had no measurable anti-rAAVrh74 antibody titer at baseline, but they showed anti-rAAVrh74 serum antibodies at 1, 2, and 3 months post-treatment, with the highest levels occurring at 3 months. At 3 months post-rAAVrh74.MCK.GALGT2 treatment, subject 07D147 showed

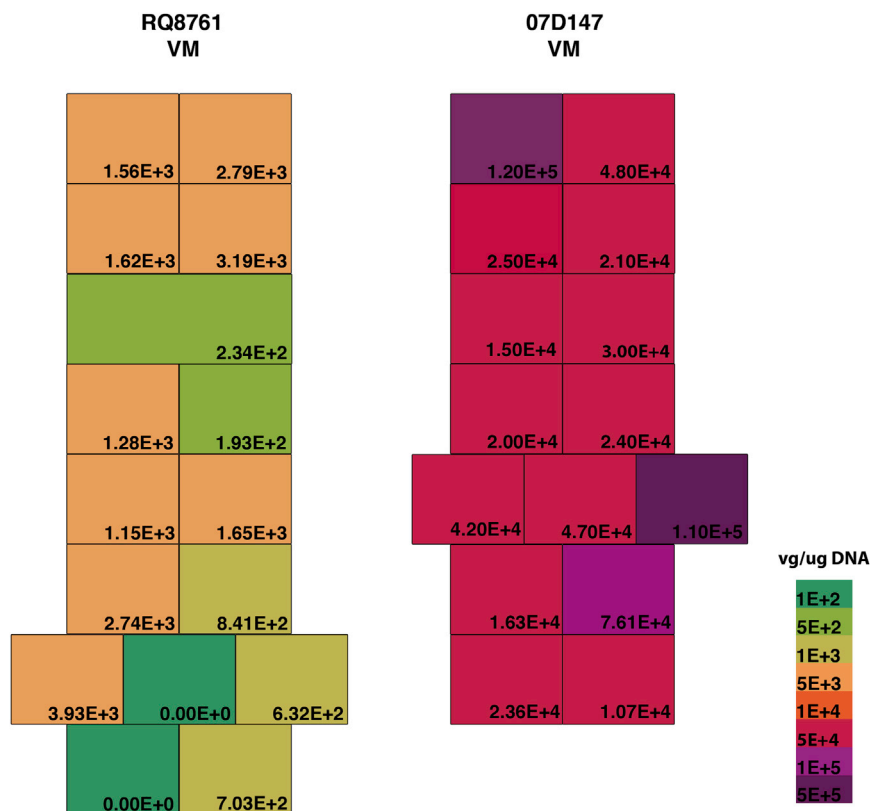


Figure 7. Heatmap of rAAVrh74.MCK.GALGT2 Vector Distribution by Dose in the Vastus Medialis Muscle following Bilateral Isolated Limb Perfusion

AAV vector genome (vg) distribution comparing the 6×10^{12} vg/kg/limb dose (left) and the 2.5×10^{13} vg/kg/limb dose (right) for the blocks taken from the VM muscle.

a positive rAAVrh74 antibody response at a 1:51,200 serum dilution and subject 04C034 showed a positive antibody response at a 1:25,600 serum dilution. Thus, rAAVrh74.MCK.GALGT2 treatment induced serum antibodies to rAAVrh74 capsid in both macaques in the months after treatment, much as has been seen previously.¹⁰

Blood Cell Counts and Serum Chemistries

Red and white blood cells counts (Table 4) and serum chemistries (Table 5), including liver enzymes, were assayed at baseline; at 24 and 48 hr post-rAAVrh74.MCK.GALGT2 treatment; and at 1, 2, and 3 months post-treatment. All blood cell counts were within the normal range for macaques of the ages used in this experiment.^{40,41} We did, however, observe a slight decrease in red blood cells, hemoglobin, and hematocrit at 24 and 48 hr post-treatment that reverted to baseline levels at 1, 2, and 3 months post-treatment. Similarly, serum chemistries (Table 5) generally were unaffected at all time points except for transient elevations in serum activities of creatine kinase, amylase, and aspartate aminotransferase (AST) at 24 and 48 hr post-treatment, all of which reverted to baseline levels at 1, 2, and 3 months post-treatment.

Assessment of Tissue Pathology

Organ blocks from subjects 07D147 and 04C034, a treated 9-year-old male and a treated 12-year-old female, and subject 07D185, a mock-

treated 5-year-old male, were fixed in formalin, processed, sectioned, and stained with H&E to evaluate tissue pathology (Table 6). Two muscle blocks, the gracilis and biceps femoris, in vector-treated subject 04C034 showed a treatment-associated anatomic finding, minimal leukocyte infiltration, presumed to be CD8+ T cells as in other studies (Figure 10).^{10,42} These leukocyte aggregates were not associated with damage (e.g., degeneration) of the adjacent myofibers. Muscle lesions were not observed in the other twelve muscle samples of the treated limb in subject 04C034, nor were lesions found in any muscle block in vector-treated subject 07D147. Other minimal findings were considered to be consistent with spontaneous background changes that occur in rhesus macaques of this age (9 or 12 years). These incidental changes included minimal mononuclear cell infiltrates in heart or lung, as well as mild inflammatory infiltrates in the bladder and moderate hepatocellular vacuolation in the liver of subject 04C034 (Table 6).

DISCUSSION

The experiments presented here describe transduction of major muscle groups throughout the leg with rAAVrh74.MCK.GALGT2 after bilateral ILI. In this method, the limb vasculature is isolated with balloon catheters in both the femoral artery and vein, within the pelvic region, for 10 min during vector delivery. Most limb muscles were significantly transduced with GALGT2 gene therapy if a dose of 2.5×10^{13} vg/kg/limb was used, which equates to a total systemic dose of 5×10^{13} vg/kg for the bilateral limb delivery. While clearly there is room for improved muscle transduction at higher doses, previous studies in mdx mice suggest that functional improvements, including both increased specific force and decreased force drop during eccentric contractions,²³ occur when only 15% or 20% of muscle fibers are transduced with rAAVrh74.MCK.GALGT2. We have undertaken a method involving bilateral limb transduction because such a protocol is anticipated to be required in clinical trials in order to improve or sustain ambulation in DMD patients. While walking is a complex process, Anderson and Pandy have modeled ambulation to show that the heel strike predominantly utilizes the ankle dorsiflexor muscles below the knee (which include the EDL and tibialis anterior [TA]), with the gluteus (maximus, minimus, and medius) and vastus (lateralis, intermedius, and medial) muscles predominating in

04C034

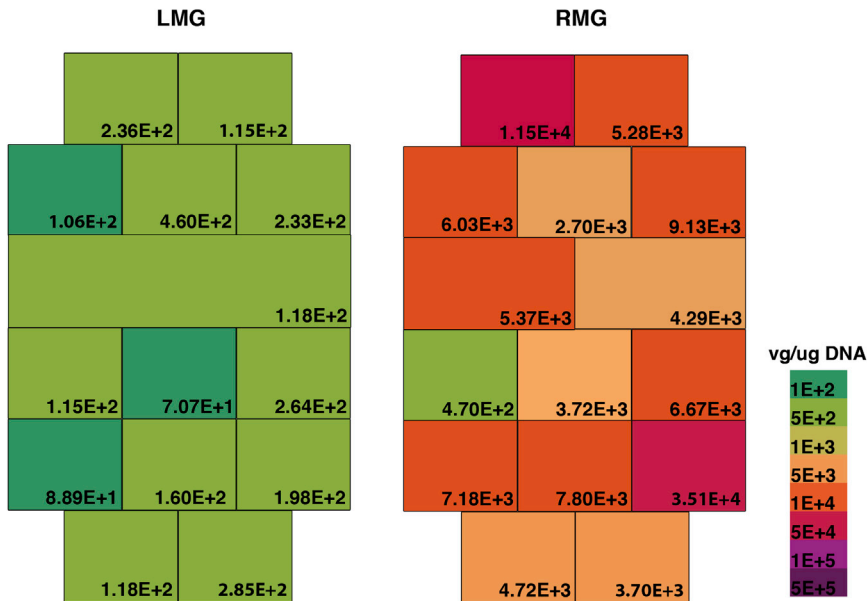


Figure 8. Heatmap of rAAVrh74.MCK.GALGT2 Vector Distribution following Single-Limb Infusion Compared to Distribution in the Contralateral Untreated Limb for the Medial Gastrocnemius Muscle

AAV vector genome (vg) distribution comparing the 6×10^{13} vg/kg/limb dose (R) and the contralateral untreated limb (L) for the blocks taken from the MG muscle.

importance when the foot is flat, while the late toe-off extension requires more work from the ankle plantarflexors (which include the medial and lateral gastrocnemius and the soleus).⁴³ We have shown that all of the muscles listed, save the gluteus muscles, reach percentages of transduction where clinical impact is theoretically possible.

While the protocol we have used isolates the limb muscles within the pelvic region, above the profunda to allow full perfusion of all muscles fed by the femoral artery (and its downstream vessels and collaterals), the protocol does not isolate the gluteus muscles, which are immediately above the isolation zone. Vector, however, does perfuse the gluteus muscles as well, with some muscle subsegments showing 18% of all myofibers as *GALGT2* positive. This presumably is due to the fact that the gluteus muscles are the most proximal muscles to the isolation zone and, therefore, they may receive vector after the balloons are deflated following the limb isolation procedure. While use of tourniquets or vascular clamps has been shown to be effective for limb muscle transduction using others transgenes in GRMD dogs, use of balloon catheters may better ensure that vascular isolation occurs above the profunda in the femoral artery and vein.^{30,31} This, in turn, may allow retrograde injection to reach more limb muscles than vascular clamps, which are often placed more caudally.

Systemic i.v. delivery of AAV in animal models can lead to effective widespread transduction of skeletal muscle in a number of species, but there are several reasons why delivery to an isolated limb would be of value.⁴⁴⁻⁴⁷ One advantage would be in the lowering of risk in early phase human clinical trials by lowering overall vector dose, which may be particularly important in protecting against hepatotox-

icity. Wilson and colleagues recently demonstrated that lethal liver toxicity can be a risk in macaques given a high (2×10^{14} vg/kg) dose of AAV.⁴⁸ To provide a clinical benefit to all muscles, i.v. delivery will require the use of such doses and perhaps even larger ones. While we did not directly compare systemic i.v. delivery and ILI in this study, several other i.v. studies in macaques have reported on AAV biodistribution in liver. For example, Fu, McCarty, and colleagues delivered a systemic i.v. dose of 2×10^{13} vg/kg rAAV9.CMV.NAGLU to macaques.⁴⁹ Using a starting dose that was 2.5 or 3 times lower than the two high doses used in our study, they reported an average of 65 vg/nucleus in the livers of 3 subjects measured at 3 months after AAV delivery. This stands in contrast to an average of 20 vg/nucleus in 2 subject livers in our 3-month study. The i.v. dosing of rAAV9.CMV.NAGLU at 2×10^{14} vg/kg, a dose 3.6 or 4 times larger than the two high doses in our ILI study, found 3.2×10^7 vg/ μ g genomic DNA in liver at 6 weeks post-treatment, in contrast to an average of 3.3×10^6 vg/ μ g for our study at 3 months post-treatment.⁵⁰ Thus, at least in these two comparisons (albeit with a different AAV serotype), there appears to be a 2.5- to 6-fold reduction in vector delivery to the liver, relative to dose, using ILI instead of i.v. delivery. Another unwanted risk is the potential of AAV genome integration into the host genome. While most AAV genomic integration events would be expected to be of no consequence, the risk of liver cancer does increase with increasing AAV dose, again making reduced liver perfusion by the ILI procedure an attractive alternative to higher systemic i.v. dosing.⁵¹

By creating a heatmap within each muscle of the leg to describe AAV biodistribution and *GALGT2*-dependent glycosylation, we now have a better understanding of the variability of AAV distribution and functional *GALGT2* expression throughout each leg muscle after ILI in a large animal model. In human trials, one muscle block is typically taken from a patient to assess transgene and protein expression. The experiments here suggest that the amount of vector loaded into that particular muscle block could vary greatly relative to other regions within the same muscle. In addition, as many as half of all muscle blocks in particular muscles may receive no detectable vector (less than 50 vg/ μ g), while other segments in the same muscle can receive 10^5 vg/ μ g genomic DNA, suggesting highly varied vascular access to subdomains of individual skeletal muscles. This large range in vector

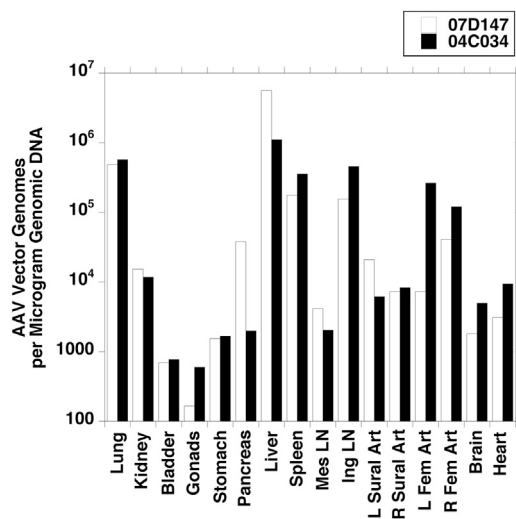


Figure 9. AAV Vector Genome Biodistribution in Organs after Vascular Delivery of rAAVrh74.MCK.GALGT2 by Isolated Limb Infusion in the Macaque

Average AAV vector genomes (vg) per microgram of genomic DNA are compared in different organs after infusion of rAAVrh74.MCK.GALGT2 in subject 07D147, a macaque that received a bilateral total dose of 5×10^{13} vg/kg (split between both legs), and subject 04C034, which received a unilateral total dose of 6×10^{13} vg/kg (all given to one leg). Assessments were done at 3 months post-treatment. LN, lymph node; Art, artery; Mes, mesenteric; Ing, inguinal.

biodistribution between treated muscles is similar to the findings of Dickson and colleagues using rAAV8.Spc5.12.MD1 (microdystrophin) in GRMD dogs.³⁰ There, an ILI method using a tourniquet was used to inject four subjects with 1×10^{13} vg/kg of rAAV in the forelimb. For muscles with >5% positive dystrophin expression, biodistribution of vector genomes between different muscles varied from about 0.003 vg/diploid genome (dg) to 5 vg/dg, or roughly 4×10^2 vg/μg to 8×10^5 vg/μg dog genomic DNA. Voit and colleagues showed a similar range of biodistribution in 13 GRMD limb muscles treated with rAAV8.U7.E6/E8, a vector designed to exon skip dystrophin, again using an ILI method with a tourniquet.²⁹ There, in four subjects dosed with 5×10^{12} vg/kg, they found rAAV muscle biodistribution ranged between about 0.02 vg/dg and 7 vg/dg, while the same protocol using a 5×10^{13} vg/kg dose (in 6 GRMD subjects) ranged between about 0.1 vg/dg and 13 vg/dg.

As in our study, both of these studies also identified expression, albeit at lower levels, in untreated limbs, demonstrating vector release into the systemic vasculature following removal of the tourniquet. Interestingly, in the Dickson study it took only one-tenth the AAV dose to achieve a high percentage of myofibers stained with microdystrophin with the ILI forelimb method as was needed with systemic i.v. dosing, suggesting concentration of vector in the limb with ILI. Our study also supports this conclusion, as we identified a 12 ± 3 -fold increase in vector genomes in a unilaterally treated limb compared to the contralateral untreated limb after vector was released from the treated limb into the systemic circulation. This differential bio-

distribution is consistent with the fact that blood circulates through the body roughly once every minute. The holding of vector in the limb vasculature for 10 minutes, with an additional minute for the post-flush, thus likely increased vector exposure to the treated limb by 11 blood perfusion cycles, which is very much in line with our measured 12 ± 3 -fold increase.

No significant safety concerns were observed using our protocol. There was a transient drop in hematocrit over the first 2 days of treatment, which may result from the volume loading during treatment. At the same time, there was a transient increase in serum activities of liver enzymes, which may be due to the amount of vector that ultimately reached this organ. Neither of these changes were linked to treatment-related tissue damage. Serum CK activity was also elevated in the first 2 days after treatment. This elevation may reflect pharmacological changes resulting from the anesthesia used, from the extended dorsal recumbency endured during the procedure, or from the procedure itself. This again was not linked to treatment-related tissue damage. The one rhesus macaque (subject 04C034) that received a high AAV dose (6×10^{13} vg/kg) in a single limb did exhibit single very small foci of mononuclear leukocytes in 2 of 14 muscles analyzed (the gracilis and biceps femoris). These foci may represent minimal inflammatory responses to AAV treatment, although no myofiber damage was seen in association with these sites. They may also reflect incidental background findings, especially given their absence in the majority of muscles analyzed from vector-treated animals. These experiments provide proof-of-concept data indicating that the use of intra-arterial and i.v. balloon catheters to isolate the limb vasculature can concentrate AAV in the limb and, thus, increase vector-derived therapeutic transgene function without eliciting significant toxicity.

MATERIALS AND METHODS

Animals

Rhesus macaques were housed and used in accordance with protocols approved by the Institutional Animal Care and Use Committee at Nationwide Children's Hospital. Indian rhesus macaques were purchased from Covance Laboratories (Princeton, NJ).

Class 1 MHC Haplotype Analysis

Expression of *Mamu-A* and *Mamu-B* macaque MHC class 1 haplotypes was determined prior to vector treatment using deep sequencing methods, as previously described, by Dr. Roger Wiseman and colleagues at the Wisconsin National Primate Research Center (Madison, WI).^{52,53}

rAAV Production

rAAVrh74.MCK.GALGT2 was made by the triple transfection method in HEK293 cells and purified using sucrose density centrifugation and anion exchange (iodixanol) chromatography by the Viral Vector Core at Nationwide Children's Hospital.^{54,55}

ILI in Rhesus Macaque

A sedated and anesthetized rhesus macaque was intubated with appropriately sized endotracheal tube and placed on assisted

Table 2. ELISpot Responses in PBMCs to rAAVrh74 Capsid and Human GALGT2 Peptides

Number of ELISpots per Million PBMCs		Control		rAAVrh74 Capsid Peptide Pool			GALGT2 Peptide Pool	
Time	Subject	ConA	DMSO	Pool 1	Pool 2	Pool 3	Pool1	Pool 2
Baseline	07D147	2,310	38	0	0	16	1	9
	04C034	1,821	0	0	0	8	0	0
1 month	07D147	1,346	0	3	0	4	0	0
	04C034	947	0	0	0	0	0	0
2 months	07D147	1,960	0	0	16	5	0	0
	04C034	1,441	0	0	0	10	0	0
3 months	07D147	1,080	0	0	0	0	0	0
	04C034	1,280	0	0	9	1	0	33

ventilation. The groin/femoral regions were prepped and draped to allow femoral vascular access. The femoral vein and artery of both legs were percutaneously entered, and an appropriately sized sidearm sheath and dilator were advanced to both vessels in a cephalic direction. A SonoSite ultrasound apparatus was used as needed to isolate the femoral vessels, and fluoroscopy was used to guide ultimate placement of the sheaths and balloon catheters, which were used to isolate the lower extremity from the central circulation. A baseline activated clotting time (ACT) level was obtained, and unfractionated heparin (Sargent Pharmaceuticals) was administered i.v. to maintain ACT levels at approximately 2 times normal baseline values. Serial ACTs were obtained every 30 min to ensure proper anticoagulation throughout the remainder of the procedure.

With fluoroscopy visualization, a 0.014 ChoICE PT coronary guidewire was inserted through the venous sheath, and a Tyshak II balloon catheter was prepped, purged, and passed over the coronary guidewire to occlude venous return from the femoral vein. A second 0.014 ChoICE PT coronary guidewire was passed through the arterial sheath, and a Tyshak mini-balloon catheter was inserted over the coronary guidewire to adjust for occlusion of the femoral artery above the femoral head, blocking vascular return to the hip, thigh, calf, and foot. After appropriate adjustment of both the venous Tyshak II balloon

and the arterial Tyshak mini-balloon catheters, confirmation of complete retrograde filling of the femoral artery (to include the hip, thigh, knee, and calf) was assessed, while the arterial and venous balloons were inflated. We performed several contrast injections that demonstrated the balloons were in the correct position.

After balloon inflation within the femoral vein and artery, a test injection of contrast was given through the sidearm of the arterial sheath to test for retrograde perfusion down the thigh, knee, calf, feet, and toes. 2 mL/kg LR solution (pre-flush) was injected through the sidearm of arterial sheath for retrograde filling of the lower extremity. The pre-flush of LR solution was infused over approximately 1 min. Next, the gene vector, pre-mixed in AAV buffer (20 mM Tris [pH 8.0], 1 mM MgCl₂, 200 mM NaCl, and 0.001% Pluronic F68) by NHC pharmacy to a total volume of 8 mL/kg in LR solution, was infused through the sidearm of the arterial sheath over 1 min. We then initiated a dwell time of 10 min for the vector containing transgene to penetrate into the lower extremity. After 10 min, an additional 2 mL/kg LR solution (post-flush) was infused through the sidearm of the arterial sheath over approximately 1 min. The balloon catheters were then deflated to reestablish arterial and venous flow, catheters and sheaths were removed, and a HemCon patch was applied to stop bleeding. There was no significant hematoma noted.

Table 3. Serum Antibody Titers to AAVrh74 Capsid at Baseline and after rAAVrh74.MCK.GALGT2 Treatment

Time	Baseline		1 Month		2 Months		3 Months	
Subject	07D147	04C034	07D147	04C034	07D147	04C034	07D147	04C034
Last point serum dilution point (positive)	<1:50	<1:50	1:6,400	1:12,800	1:51,200	1:12,800	1:51,200	1:25,600
Ratio of sample to background (>2 is positive)	0.4	1.4	2.9	3.0	2.8	2.4	2.0	2.0
First serum dilution point (negative)	NA	NA	1:12,800	1:25,600	1:102,400	1:25,600	1:102,400	1:51,200
Ratio of sample to background (negative)	NA	NA	1.6	1.5	1.3	1.5	0.8	1.1
Positive control (ratio of sample to background)	14.7	21.0	10.3	10.3	7.7	10.9	8.0	8.4
Negative control (ratio of sample to background)	0.2	0.5	0.3	0.3	0.2	0.2	0.2	0.4

NA, not applicable.

Table 4. Hematology Measures at Baseline and after RAAVrh74.MCK.GALGT2 Treatment

Time	Subject	WBC		RBC		HGB (g/dL)	HCT (%)	MCV (fL)	MCH (pg)	MCHC (%)	RDW (%)	PLC (K/mm ³)	MPV (fL)	Neut (%)	Lymph (%)	Mono (%)	EOS (%)	BAS (%)
		(K/mm ³)	(M/mm ³)	(M/mm ³)	(M/mm ³)													
Baseline	07D147	4.2	5.06	11.7	37.1	73.3	23.1	31.5	13.3	284	11.5	47	45	8	0	0	1	
	04C034	6.2	5.94	12.9	42.7	71.9	21.7	30.2	12.2	381	10.4	71	23	0	0	0	0	
24 hr	07D147	4	3.67	8.5	26.5	72.2	23.2	32.1	13.3	128	12.3	77	19	2	0	2		
	04C034	5.2	3.67	8.0	26.3	71.7	21.8	30.4	12.4	218	11.2	73	16	10	1	0		
48 hr	07D147	4.6	3.16	7.3	23.4	74.1	23.1	31.2	13.4	157	11.6	52	37	7	0	3		
	04C034	3.3	3.56	7.6	25.8	72.5	21.3	29.5	12.1	222	11.0	53	29	9	9	0		
1 month	07D147	4.1	5.71	12.9	42.4	74.3	22.6	30.4	13.2	296	10.6	49	45	6	0	0		
	04C034	5.2	5.91	12.8	42.2	71.4	21.7	30.3	12.5	297	11.5	68	25	6	0	1		
2 months	07D147	4.4	6.18	13.7	45.2	73.1	22.2	30.3	13.2	256	10.7	48	46	6	0	0		
	04C034	5.5	6.11	13.3	43.2	70.7	21.8	30.8	12.2	426	10.2	63	32	4	0	0		
3 months	07D147	3.4	5.67	13	40	70.5	22.9	32.5	13.5	240	11.7	43	49	8	1	0		
	04C034	8.2	6.26	13.5	43.5	69.5	21.6	31	12.8	193	11.5	64	30	5	0	0		

WBC, white blood cell; RBC, red blood cell; HGB, hemoglobin; HCT, hematocrit; MCV, mean corpuscular volume; MCH, mean corpuscular hemoglobin; MCHC, mean corpuscular hemoglobin concentration; RDW, red cell distribution width; PLC, platelet count; MPV, mean platelet volume; Neut, neutrophils (relative); Lymph, lymphocytes (relative); Mono, monocytes (relative); EOS, eosinophils (relative); BAS, basophils (relative).

After recovery, animals were returned to their normal housing. In subjects with planned bilateral limb delivery, the femoral vessels of both limbs were accessed percutaneously with vascular sheaths prior to heparinization. Once access was obtained and systemic heparinization was completed as described above, one limb was treated at a time. There were no hemodynamic changes during or following the procedure. No changes in leg perfusion or color were observed post-procedure.

Assessment of GALGT2-Induced Glycosylation

The β 1,4-linked GalNAc structures made by GALGT2 were identified in tissue sections using the β GalNAc-binding lectin WFA. Muscles were dissected, cut into blocks using a map of their rostral-caudal and medial-lateral position within each skeletal muscle, snap-frozen in liquid nitrogen-cooled isopentane, sectioned at 10 μ m on a cryostat, and mounted onto slides. Sections were first blocked in PBS (pH 7.4) containing 10% donkey serum for 1 hr at room temperature. Sections were then incubated with rat anti-human/mouse laminin α 2 monoclonal antibody (clone 4H8-2, Sigma) for 1 hr at room temperature. After three 15-min washes in PBS, sections were incubated with donkey anti-rat (immunoglobulin G [IgG]) secondary antibody conjugated to Cy3 (Jackson ImmunoResearch, West Gove, PA) and 1.2 μ g/mL WFA-conjugated to FITC (fluorescein isothiocyanate) (Vector Laboratories, Burlingame, CA) for 1 hr at room temperature. After three 15-min washes in PBS, sections were dried and mounted in ProLong Gold Anti-fade mounting medium (Molecular Probes, Eugene, OR). Staining was visualized for laminin α 2 and WFA using appropriate optical filters on a Zeiss Axioskop epifluorescence microscope. For each section, 10 \times -objective images were converted in ImageJ and quantified for the percentage of GALGT2-overexpressing WFA-positive muscle fibers relative to all laminin α 2-positive myofibers, as previously described.⁴² All immunofluorescence staining was visualized with a Zeiss Axioskop2 Plus epifluorescence microscope using fluorophore-specific filters, and representative images were captured with a Zeiss AxioCam MRC5 camera (Carl Zeiss Microscopy, Jena, Germany). All images comparing individual stains were time matched using identical exposure settings across different experimental conditions.

Assessment of Heart and Fiber Type Staining

For heart immunostaining, 10 μ m cryostat-cut frozen unfixed sections were mounted on slides and blocked in 10% goat serum in PBS at room temperature for 1 hr, after which they were incubated overnight at 4°C with rabbit anti-N-cadherin polyclonal antibody (Thermo Fisher Scientific, Waltham, MA). Sections were incubated with fluorescein-labeled WFA (Vector Laboratories, Burlingame, CA) and Cy3-conjugated goat anti-rabbit secondary antibody (Jackson ImmunoResearch, West Grove, PA) for 1 hr at room temperature. After washing, sections were mounted in cover glass using ProLong Diamond Antifade Mountant (Invitrogen, Carlsbad, CA). Numbers of WFA-positive and N-cadherin-positive stained intercalated disks were measured from 10 \times fluorescent images, which were converted to black and white in NIH ImageJ (ImageJ 1.46). Positive staining was quantified using Analyze Particles mode. For

Table 5. Blood Chemistries before and after Treatment with rAAVrh74.MCK.GALGT2

Time	Subject	Albumin (g/dL)	ALP (U/L)	ALT (U/L)	Amylase (U/L)	AST (U/L)	BUN (mg/dL)	CK (U/L)	Creatinine (mg/dL)	Glucose (mg/dL)	Osmolality (mosmol/kg)
Baseline	07D147	3.4	82	155	278	52	13	216	1.15	57	308
	04C034	3.6	106	31	362	30	16	136	0.87	59	313
24 hr	07D147	3	56	200	745	365	13	7,880	0.98	86	306
	04C034	2.6	98	118	3,820	283	23	5,581	1.04	83	312
48 hr	07D147	3	62	190	471	208	10	2,949	0.89	78	307
	04C034	2.8	147	117	1,479	157	11	928	0.81	97	306
1 month	07D147	3.9	79	141	278	43	19	78	1.12	76	309
	04C034	3.7	119	35	299	38	12	120	0.81	45	309
2 months	07D147	4.1	62	193	269	116	17	225	0.95	69	301
	04C034	3.6	127	40	332	27	15	63	0.82	59	296
3 months	07D147	3.9	65	170	229	71	14	208	1.1	65	301
	04C034	3.3	133	55	307	33	13	66	0.76	59	306

ALP, alkaline phosphatase; ALT, alanine aminotransferase; AST, aspartate aminotransferase; BUN, blood urea nitrogen; CK, creatine kinase.

subject 07D147, three blocks of left ventricle, four blocks of right ventricle, and two blocks of right atrium were used for analysis (total of 3,617 intercalated disks). For subject RQ8761, two ventricle blocks were used for analysis (total of 1,041 intercalated disks).

Unfixed skeletal muscle tissues were mounted and snap-frozen in liquid nitrogen-cooled isopentane and sectioned at 10 μ m. Fiber-type immunostaining was done using antibodies purchased from Developmental Studies Hybridoma Bank (Iowa City, IA). Antibody A4.840 specific to type 1 fibers, antibody 2F7 specific to type 2A fibers, antibody 6H1 specific to type 2X fibers, and antibody F18 specific to type 2B fibers were used to identify muscle fiber types. Rat anti-laminin α 2 antibody (4H8, Sigma-Aldrich, St. Louis, MO) staining was used as a counterstain to identify all myofibers, and fluorescein-conjugated WFA (Vector Laboratories, Burlingame, CA) was used to identify *GALGT2*-overexpressing myofibers. Cy3-conjugated goat anti-mouse and Cy5-conjugated goat anti-rat secondary antibodies were used to identify fiber type and laminin α 2 staining, respectively (Jackson ImmunoResearch, West Grove, PA). After staining, slides were mounted in cover glass using ProLong Diamond Antifade Mountant (Invitrogen, Carlsbad, CA). Cell counts were done using ImageJ software (ImageJ 1.46r, NIH) with the Cell Counter plugin, with the green channel image used to confirm WFA-positive cells and the red channel image used to confirm fiber type antibody-expressing cells. 2 blocks per muscle and per condition were used, with 5 $10\times$ images counted in their entirety for each sample. All immunofluorescence staining was visualized with a Zeiss Axioskop2 Plus epifluorescence microscope using fluorophore-specific filters, and representative images were captured with a Zeiss AxioCam MRC5 camera (Carl Zeiss Microscopy, Jena, Germany). All images comparing individual stains were time matched using identical exposure settings across different experimental conditions.

Serum Anti-rAAVrh74 ELISAs

Serum ELISAs for rAAVrh74 capsid protein were done and analyzed as previously described.⁴² rAAVrh74 was provided by the Viral Vector Core Facility at NCH. A rabbit anti-rhesus macaque IgG secondary antibody linked to horseradish peroxidase (HRP) was purchased from Sigma-Aldrich (St. Louis, MO). Briefly, 2×10^9 vg rAAVrh74 was coated on each well of a 96-well ELISA plate (Immulon 4HBX, Thermo Scientific, Carlsbad, CA) in 0.2 M bicarbonate buffer (pH 9.4) overnight at 4°C for positive wells. Control wells were incubated with bicarbonate buffer without rAAVrh74. All subsequent steps were done at 37°C. Plates were washed and then blocked in blocking solution (PBS with 5% non-fat dry milk and 1% goat serum) for 2–3 hr. Macaque serum, diluted with PBS beginning at 1:50 and then sequentially diluted in 1:2 increments thereafter, was added to wells for 1 hr. We had previously shown that the presence of positive total serum antibodies at a dilution of 1:800, or 16 times our pre-screening negative value, was required to block macaque skeletal myofiber transduction by rAAVrh74.MCK.GALGT2 after intra-arterial delivery.¹⁰ Note that these ELISA measures reflect total anti-rh74 antibody titer and not neutralizing antibody titer. After washing, plates were incubated with rabbit anti-rhesus macaque IgG-HRP for 30 min, washed, developed for 15 min with TMB (3,3',5,5'-tetramethylbenzidine) HRP color substrate, quenched in 1 N sulfuric acid, and read on a Bio-Tek Synergy 2 plate reader at 450 nm for absorbance. Only wells where serum bound to rAAVrh74 gave a signal that was 2-fold or more above the background-subtracted signal were considered to be positive for any given serum dilution.

GALGT2 and rAAVrh74 Capsid ELISpot Assays

ELISpot assays were performed on PBMCs, which were added at 2×10^5 cells/well to duplicate wells of a polyvinylidene fluoride (PVDF)-coated 96-well plate (MSIP S4520, Millipore). For each

Table 6. Summary of Tissue Pathology Findings 3 Months after Treatment with rAAVrh74.MCK.GALGT2

Subject (Total Dose)	07D185 (Control)	07D147 (5E+13 vg/kg)	04C034 (6E+13 vg/kg)
Femoral artery left and right	-	-	-
Sural artery left and right	-	-	-
Gonad	- (testis)	- (testis)	- (ovary)
Kidney	infiltration, lymphocytic, perivascular, focal, mild, cortex	-	-
Urinary bladder	-	infiltrate, mononuclear cell, focal, minimal	-
Lung	-	-	infiltrate, mononuclear cell, multifocal, minimal
Pancreas	-	-	-
Spleen	-	-	-
Stomach	-	-	inflammation, plasmacytic, diffuse, mild
Liver	-	infiltrate, mononuclear cell, multifocal, minimal	vacuolation, hepatocellular, diffuse, moderate (consistent with glycogen)
Heart ^a	-	-	left ventricle, infiltrate, mononuclear cell, multifocal, minimal,
Diaphragm	-	-	-
Skeletal muscle ^b	-	-	-
Skeletal muscle ^c	-	-	infiltrate, mixed cell (macrophages mainly), multifocal, minimal
Skeletal muscle ^d	-	-	infiltrate, mononuclear cell, focal, minimal

Lesion scores: dash, within normal limits.

^aAtria and ventricles (free walls).

^bBiceps brachii, biceps femoris, extensor digitorum longus, gastrocnemius (medial and lateral), gluteus (maximus, medius, and minimus), gracilis, rectus femoris, sartorius, semimembranosus, semitendinosus, soleus, triceps brachii, tibialis anterior, and vastus (intermedius, lateralis, and medialis).

^cRight biceps femoris.

^dRight gracilis.

well, 0.2 µg peptides from one of three peptide pools to rAAVrh74 capsid protein sequence or one of two pools of GALGT2 protein sequence were then added. Overlapping peptide pools of 18 amino acids in length to the rAAVrh74 capsid protein or the human GALGT2 protein were assayed as previously described.⁴² 2 µg ConA was added to PBMCs as a positive control, and vehicle (0.25% DMSO) was used as a negative control. Peptides were added at 1 mg/mL to Aim-V lymphocyte media (Life Technologies, Grand Island, NY) supplemented with 2% human AB serum (Gemini-BioScience, Liverpool, UK). Monkey interferon (IFN)-γ ELISpot kits were purchased from U-CyTech (Utrecht, the Netherlands). After the addition of PBMCs and peptides, the plates were incubated at 37°C for 48 hr in a tissue culture incubator with 5% CO₂, and plates were then developed according to the manufacturer's instructions for IFN-γ signal. Spot formation was counted using a Cellular Technologies Systems analyzer (Cleveland, OH).

qPCR Measures of rAAV Vector Biodistribution

Organs were snap-frozen in blocks in liquid nitrogen, except for skeletal muscles, which were mounted and frozen in liquid nitrogen-cooled isopentane, after which shavings were collected after cutting on cryostat. TaqMan qPCR was used to quantify AAV vector genomes, as previously described.^{10,42} Genomic DNA was extracted

from all blocks taken from each limb skeletal muscle. DNA purity and quantity were measured using an ND-1000 spectrophotometer (Thermo Scientific, Carlsbad, CA). A vector-specific probe set (forward 5'-CCTCAGTGGATGTTGCCTTTA-3', probe 5'-AAAGCTGCG/ZEN/GAATTGTACCCGC/3IABkFQ-3', and reverse 5'-ATCTTGAGGAGCCACAGAAATC-3') was used to amplify a portion of the vector DNA encompassing the 3' end of the MCK promoter and the 5' end of the human GALGT2 cDNA. No amplification of the endogenous macaque (*Macaca mulatta*) GALGT2 was observed in control samples. Copy number is reported as vector genomes per microgram of genomic DNA assayed relative using linear pAAV.MCK.GALGT2 plasmid between 50 and 50 million copies as a linear standard. Differences between the cohorts were analyzed using an ordinary one-way ANOVA and Sidak's multiple comparisons test. Addition of plasmid (spike-ins) to genomic skeletal muscle DNA was done to confirm lack of signal quenching by genomic DNA.

Histopathology

Non-muscle tissues were fixed in neutral buffered formalin, processed routinely in paraffin, sectioned, and stained with H&E, as previously described.³⁴ Unfixed skeletal muscle tissues were mounted and snap-frozen in liquid nitrogen-cooled isopentane, sectioned at

07D147 R BF

04C034 R BF

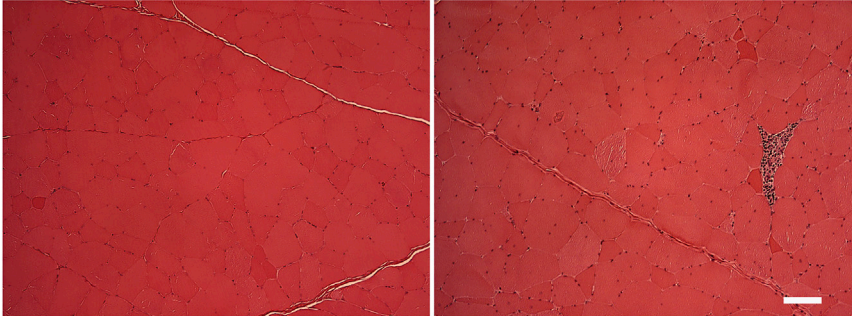


Figure 10. Leukocyte Infiltration in Skeletal Muscle following rAAVrh74.MCK.GALGT2 Delivery by Isolated Limb Infusion

The biceps femoris muscle in the right leg (R BF) from subject 04C034, which received a dose of 6×10^{13} vg/kg/limb rAAVrh74.MCK.GALGT2, showed minimal mononuclear cell infiltration in the absence of myofiber damage, while subject 07D147, which received a dose of 2.5×10^{13} vg/kg/limb, did not have such changes. H&E staining. Scale bar, 100 μ m.

10 μ m, and stained with H&E. Unfixed cardiac muscle was submerged in mounting medium, frozen in dry ice-cooled isopentane, sectioned at 10 μ m, and stained with H&E. Tissues were then analyzed independently for pathological findings. Semiquantitative grading pathological changes in muscle and non-muscle tissues included the following categories: within normal limits (0% of tissue), minimal (<5% and >0% of tissue), mild (5%–15% of tissue), moderate (>15%–40% of tissue), and marked (>40% of tissue).

Serum Chemistries

Whole blood was collected, serum was separated from clotted blood cells, and serum chemistries were measured as previously described.³⁴

SUPPLEMENTAL INFORMATION

Supplemental Information includes one figure and can be found with this article online at <https://doi.org/10.1016/j.omtm.2018.06.002>.

AUTHOR CONTRIBUTIONS

R.X. initiated and oversaw the project design, interpreted and analyzed all primary data, and aided in writing the manuscript. Y.J., D.A.Z., M.L.C., K.E.C., G.S., A.E.M., H.N.G., and B.C.H. were all involved in the quantification of skeletal muscle heatmap expression. Y.J. and D.A.Z. were also involved in the quantification of heart and fiber type expression. R.X., D.A.Z., D.A.G., and E.P. were involved in the necropsies and organ preparations. R.X. performed ELISpot analysis. D.A.Z. performed serum ELISAs. R.X., Y.J., D.A.Z., and G.S. were involved in biodistribution analysis. B.B. was responsible for the analysis of tissue histopathology. J.P.C., S.L.C., and L.G.C. performed the ILI procedures. L.R.R.-K. provided analysis and funding for necropsies. B.B., J.P.C., S.L.C., K.M.F., L.R.R.-K., and L.G.C. advised and were involved in editing the manuscript. P.T.M. conceptualized and designed the project, obtained funding along with K.M.F. for the project, contributed to data analysis, and along with R.X. and D.A.Z. wrote the manuscript.

CONFLICTS OF INTEREST

P.T.M. is the inventor of rAAVrh74.MCK.GALGT2 and receives licensing fees for its use from a biotechnology company. As such, he has a financial conflict of interest in the publication of this work. None of the other authors have any conflicts to report.

ACKNOWLEDGMENTS

This study was supported by NIH grant R01 AR049722 (to P.T.M.), a Center of Research Translation NIH grant (P50 AR070604 to K.F.M.), and the Nationwide Children's Hospital Foundation. Production of the toxicology grade lot of rAAVrh74.MCK.GALGT2 was supported by NIH grant U54 NS055958 (to P.T.M.). K.E.C. was supported, in part, by the Seilhamer Fellowship from the Jeffery J. Seilhamer Cancer Foundation, and M.L.C. was supported, in part, by T32 NIH training award T32 NS077984. Special thanks to Kristin Heller, Ryan Johnson, Rachael Potter, Eric Pozsgai, Chrystal Montgomery, and Kim Shontz (all NCH) for help with tissue and organ dissections and to Nianyaun Huang and Felicia Gumienny (NCH) for assistance with sample processing. Special thanks to Dr. Roger Wiseman and colleagues at the Wisconsin National Primate Research Center (Madison, WI) for *Mamu-A* and *Mamu-B* haplotype expression analysis.

REFERENCES

- Mingozzi, F., and High, K.A. (2013). Immune responses to AAV vectors: overcoming barriers to successful gene therapy. *Blood* 122, 23–36.
- High, K.A., and Anguela, X.M. (2016). Adeno-associated viral vectors for the treatment of hemophilia. *Hum. Mol. Genet.* 25 (R1), R36–R41.
- Spencer, H.T., Riley, B.E., and Doering, C.B. (2016). State of the art: gene therapy of haemophilia. *Haemophilia* 22 (Suppl 5), 66–71.
- Calcedo, R., and Wilson, J.M. (2013). Humoral Immune Response to AAV. *Front. Immunol.* 4, 341.
- Wang, Z., Tapscott, S.J., Chamberlain, J.S., and Storb, R. (2011). Immunity and AAV-Mediated Gene Therapy for Muscular Dystrophies in Large Animal Models and Human Trials. *Front. Microbiol.* 2, 201.
- Tichet, J., Vol, S., Goxe, D., Salle, A., Berrut, G., and Ritz, P. (2008). Prevalence of sarcopenia in the French senior population. *J. Nutr. Health Aging* 12, 202–206.
- Findlay, A.R., Wein, N., Kaminoh, Y., Taylor, L.E., Dunn, D.M., Mendell, J.R., King, W.M., Pestronk, A., Florence, J.M., Mathews, K.D., et al.; United Dystrophinopathy Project (2015). Clinical phenotypes as predictors of the outcome of skipping around DMD exon 45. *Ann. Neurol.* 77, 668–674.
- Wein, N., Alfano, L., and Flanigan, K.M. (2015). Genetics and emerging treatments for Duchenne and Becker muscular dystrophy. *Pediatr. Clin. North Am.* 62, 723–742.
- Xu, R., Camboni, M., and Martin, P.T. (2007). Postnatal overexpression of the CT GalNAc transferase inhibits muscular dystrophy in mdx mice without altering muscle growth or neuromuscular development: evidence for a utrophin-independent mechanism. *Neuromuscul. Disord.* 17, 209–220.
- Chicoine, L.G., Rodino-Klapac, L.R., Shao, G., Xu, R., Bremer, W.G., Camboni, M., Golden, B., Montgomery, C.L., Shontz, K., Heller, K.N., et al. (2014). Vascular

- delivery of rAAVrh74.MCK.GALGT2 to the gastrocnemius muscle of the rhesus macaque stimulates the expression of dystrophin and laminin $\alpha 2$ surrogates. *Mol. Ther.* 22, 713–724.
11. Xu, R., Chandrasekharan, K., Yoon, J.H., Camboni, M., and Martin, P.T. (2007). Overexpression of the cytotoxic T cell (CT) carbohydrate inhibits muscular dystrophy in the dyW mouse model of congenital muscular dystrophy 1A. *Am. J. Pathol.* 171, 181–199.
 12. Nguyen, H.H., Jayasinha, V., Xia, B., Hoyte, K., and Martin, P.T. (2002). Overexpression of the cytotoxic T cell GalNAc transferase in skeletal muscle inhibits muscular dystrophy in mdx mice. *Proc. Natl. Acad. Sci. USA* 99, 5616–5621.
 13. Xu, R., DeVries, S., Camboni, M., and Martin, P.T. (2009). Overexpression of Galgt2 reduces dystrophic pathology in the skeletal muscles of alpha sargoglycan-deficient mice. *Am. J. Pathol.* 175, 235–247.
 14. Thomas, P.J., Xu, R., and Martin, P.T. (2016). B4GALNT2 (GALGT2) Gene Therapy Reduces Skeletal Muscle Pathology in the FKR P448L Mouse Model of Limb Girdle Muscular Dystrophy 2I. *Am. J. Pathol.* 186, 2429–2448.
 15. Xia, B., Hoyte, K., Kammesheidt, A., Deerinck, T., Ellisman, M., and Martin, P.T. (2002). Overexpression of the CT GalNAc transferase in skeletal muscle alters myofiber growth, neuromuscular structure, and laminin expression. *Dev. Biol.* 242, 58–73.
 16. Raith, M., Valencia, R.G., Fischer, I., Orthofer, M., Penninger, J.M., Spuler, S., Rezniczek, G.A., and Wiche, G. (2013). Linking cytoarchitecture to metabolism: sarcolemma-associated plectin affects glucose uptake by destabilizing microtubule networks in mdx myofibers. *Skelet. Muscle* 3, 14.
 17. Deconinck, N., Tinsley, J., De Backer, F., Fisher, R., Kahn, D., Phelps, S., Davies, K., and Gillis, J.M. (1997). Expression of truncated utrophin leads to major functional improvements in dystrophin-deficient muscles of mice. *Nat. Med.* 3, 1216–1221.
 18. Deconinck, A.E., Rafael, J.A., Skinner, J.A., Brown, S.C., Potter, A.C., Metzinger, L., Watt, D.J., Dickson, J.G., Tinsley, J.M., and Davies, K.E. (1997). Utrophin-dystrophin-deficient mice as a model for Duchenne muscular dystrophy. *Cell* 90, 717–727.
 19. Grady, R.M., Teng, H., Nichol, M.C., Cunningham, J.C., Wilkinson, R.S., and Sanes, J.R. (1997). Skeletal and cardiac myopathies in mice lacking utrophin and dystrophin: a model for Duchenne muscular dystrophy. *Cell* 90, 729–738.
 20. Tinsley, J., Deconinck, N., Fisher, R., Kahn, D., Phelps, S., Gillis, J.M., and Davies, K. (1998). Expression of full-length utrophin prevents muscular dystrophy in mdx mice. *Nat. Med.* 4, 1441–1444.
 21. Moll, J., Barzaghi, P., Lin, S., Bezakova, G., Lochmüller, H., Engvall, E., Müller, U., and Ruegg, M.A. (2001). An agrin minigene rescues dystrophic symptoms in a mouse model for congenital muscular dystrophy. *Nature* 413, 302–307.
 22. Reinhard, J.R., Lin, S., McKee, K.K., Meinen, S., Crosson, S.C., Sury, M., Hobbs, S., Maier, G., Yurchenko, P.D., and Ruegg, M.A. (2017). Linker proteins restore basement membrane and correct LAMA2-related muscular dystrophy in mice. *Sci. Transl. Med.* 9, eaal4649.
 23. Martin, P.T., Xu, R., Rodino-Klapac, L.R., Oglesbay, E., Camboni, M., Montgomery, C.L., Shontz, K., Chicoine, L.G., Clark, K.R., Sahenk, Z., et al. (2009). Overexpression of Galgt2 in skeletal muscle prevents injury resulting from eccentric contractions in both mdx and wild-type mice. *Am. J. Physiol. Cell Physiol.* 296, C476–C488.
 24. Greelish, J.P., Su, L.T., Lankford, E.B., Burkman, J.M., Chen, H., König, S.K., Mercier, I.M., Desjardins, P.R., Mitchell, M.A., Zheng, X.G., et al. (1999). Stable restoration of the sarcoglycan complex in dystrophic muscle perfused with histamine and a recombinant adeno-associated viral vector. *Nat. Med.* 5, 439–443.
 25. Cho, W.K., Ebihara, S., Nalbantoglu, J., Gilbert, R., Massie, B., Holland, P., Karpati, G., and Petrof, B.J. (2000). Modulation of Starling forces and muscle fiber maturity permits adenovirus-mediated gene transfer to adult dystrophic (mdx) mice by the intravascular route. *Hum. Gene Ther.* 11, 701–714.
 26. Budker, V., Zhang, G., Danko, I., Williams, P., and Wolff, J. (1998). The efficient expression of intravascularly delivered DNA in rat muscle. *Gene Ther.* 5, 272–276.
 27. Wang, Z., Storb, R., Halbert, C.L., Banks, G.B., Butts, T.M., Finn, E.E., Allen, J.M., Miller, A.D., Chamberlain, J.S., and Tapscott, S.J. (2012). Successful regional delivery and long-term expression of a dystrophin gene in canine muscular dystrophy: a pre-clinical model for human therapies. *Mol. Ther.* 20, 1501–1507.
 28. Galindo, C.L., Soslow, J.H., Brinkmeyer-Langford, C.L., Gupte, M., Smith, H.M., Sengsayadeth, S., Sawyer, D.B., Benson, D.W., Kornegay, J.N., and Markham, L.W. (2016). Translating golden retriever muscular dystrophy microarray findings to novel biomarkers for cardiac/skeletal muscle function in Duchenne muscular dystrophy. *Pediatr. Res.* 79, 629–636.
 29. Le Guiner, C., Montus, M., Servais, L., Cherel, Y., Francois, V., Thibaud, J.L., Wary, C., Matot, B., Larcher, T., Guigand, L., et al. (2014). Forelimb treatment in a large cohort of dystrophic dogs supports delivery of a recombinant AAV for exon skipping in Duchenne patients. *Mol. Ther.* 22, 1923–1935.
 30. Le Guiner, C., Servais, L., Montus, M., Larcher, T., Fraysse, B., Moullec, S., Allais, M., François, V., Dutilleul, M., Malerba, A., et al. (2017). Long-term microdystrophin gene therapy is effective in a canine model of Duchenne muscular dystrophy. *Nat. Commun.* 8, 16105.
 31. Gregorevic, P., Schultz, B.R., Allen, J.M., Halldorson, J.B., Blankinship, M.J., Meznarich, N.A., Kuhr, C.S., Doremus, C., Finn, E., Liggitt, D., and Chamberlain, J.S. (2009). Evaluation of vascular delivery methodologies to enhance rAAV6-mediated gene transfer to canine striated musculature. *Mol. Ther.* 17, 1427–1433.
 32. Arruda, V.R., Stedman, H.H., Haurigot, V., Buchlis, G., Baila, S., Favaro, P., Chen, Y., Franck, H.G., Zhou, S., Wright, J.F., et al. (2010). Peripheral transvenular delivery of adeno-associated viral vectors to skeletal muscle as a novel therapy for hemophilia B. *Blood* 115, 4678–4688.
 33. Rodino-Klapac, L.R., Montgomery, C.L., Mendell, J.R., and Chicoine, L.G. (2011). AAV-mediated gene therapy to the isolated limb in rhesus macaques. *Methods Mol. Biol.* 709, 287–298.
 34. Chicoine, L.G., Montgomery, C.L., Bremer, W.G., Shontz, K.M., Griffin, D.A., Heller, K.N., Lewis, S., Malik, V., Grose, W.E., Shilling, C.J., et al. (2014). Plasmapheresis eliminates the negative impact of AAV antibodies on microdystrophin gene expression following vascular delivery. *Mol. Ther.* 22, 338–347.
 35. Fan, Z., Kocis, K., Valley, R., Howard, J.F., Jr., Chopra, M., Chen, Y., An, H., Lin, W., Muenzer, J., and Powers, W. (2015). High-Pressure Transvenous Perfusion of the Upper Extremity in Human Muscular Dystrophy: A Safety Study with 0.9% Saline. *Hum. Gene Ther.* 26, 614–621.
 36. Salva, M.Z., Himeda, C.L., Tai, P.W., Nishiuchi, E., Gregorevic, P., Allen, J.M., Finn, E.E., Nguyen, Q.G., Blankinship, M.J., Meuse, L., et al. (2007). Design of tissue-specific regulatory cassettes for high-level rAAV-mediated expression in skeletal and cardiac muscle. *Mol. Ther.* 15, 320–329.
 37. McNally, E.M. (2007). New approaches in the therapy of cardiomyopathy in muscular dystrophy. *Annu. Rev. Med.* 58, 75–88.
 38. Mays, T.A., Binkley, P.F., Lesinski, A., Doshi, A.A., Quale, M.P., Margulies, K.B., Janssen, P.M., and Rafael-Fortney, J.A. (2008). Claudin-5 levels are reduced in human end-stage cardiomyopathy. *J. Mol. Cell. Cardiol.* 45, 81–87.
 39. Xu, R., Singhal, N., Serinagaoglu, Y., Chandrasekharan, K., Joshi, M., Bauer, J.A., Janssen, P.M., and Martin, P.T. (2015). Deletion of Galgt2 (B4Galnt2) reduces muscle growth in response to acute injury and increases muscle inflammation and pathology in dystrophin-deficient mice. *Am. J. Pathol.* 185, 2668–2684.
 40. Lee, J.I., Shin, J.S., Lee, J.E., Jung, W.Y., Lee, G., Kim, M.S., Park, C.G., and Kim, S.J. (2012). Reference values of hematology, chemistry, electrolytes, blood gas, coagulation time, and urinalysis in the Chinese rhesus macaques (*Macaca mulatta*). *Xenotransplantation* 19, 244–248.
 41. Andrade, M.C., Ribeiro, C.T., Silva, V.F., Molinaro, E.M., Gonçalves, M.A., Marques, M.A., Cabello, P.H., and Leite, J.P. (2004). Biologic data of *Macaca mulatta*, *Macaca fascicularis*, and *Saimiri sciureus* used for research at the Fiocruz primate center. *Mem. Inst. Oswaldo Cruz* 99, 581–589.
 42. Cramer, M.L., Shao, G., Rodino-Klapac, L.R., Chicoine, L.G., and Martin, P.T. (2017). Induction of T-Cell Infiltration and Programmed Death Ligand 2 Expression by Adeno-Associated Virus in Rhesus Macaque Skeletal Muscle and Modulation by Prednisone. *Hum. Gene Ther.* 28, 493–509.
 43. Anderson, F.C., and Pandy, M.G. (2003). Individual muscle contributions to support in normal walking. *Gait Posture* 17, 159–169.
 44. Wang, Z., Zhu, T., Qiao, C., Zhou, L., Wang, B., Zhang, J., Chen, C., Li, J., and Xiao, X. (2005). Adeno-associated virus serotype 8 efficiently delivers genes to muscle and heart. *Nat. Biotechnol.* 23, 321–328.
 45. Bostick, B., Ghosh, A., Yue, Y., Long, C., and Duan, D. (2007). Systemic AAV-9 transduction in mice is influenced by animal age but not by the route of administration. *Gene Ther.* 14, 1605–1609.

46. Yue, Y., Ghosh, A., Long, C., Bostick, B., Smith, B.F., Kornegay, J.N., and Duan, D. (2008). A single intravenous injection of adeno-associated virus serotype-9 leads to whole body skeletal muscle transduction in dogs. *Mol. Ther.* *16*, 1944–1952.
47. Kornegay, J.N., Li, J., Bogan, J.R., Bogan, D.J., Chen, C., Zheng, H., Wang, B., Qiao, C., Howard, J.F., Jr., and Xiao, X. (2010). Widespread muscle expression of an AAV9 human mini-dystrophin vector after intravenous injection in neonatal dystrophin-deficient dogs. *Mol. Ther.* *18*, 1501–1508.
48. Hinderer, C., Katz, N., Buza, E.L., Dyer, C., Goode, T., Bell, P., Richman, L.K., and Wilson, J.M. (2018). Severe Toxicity in Nonhuman Primates and Piglets Following High-Dose Intravenous Administration of an Adeno-Associated Virus Vector Expressing Human SMN. *Hum. Gene Ther.* *29*, 285–298.
49. Murrey, D.A., Naughton, B.J., Duncan, F.J., Meadows, A.S., Ware, T.A., Campbell, K.J., Bremer, W.G., Walker, C.M., Goodchild, L., Bolon, B., et al. (2014). Feasibility and safety of systemic rAAV9-hNAGLU delivery for treating mucopolysaccharidosis IIIB: toxicology, biodistribution, and immunological assessments in primates. *Hum. Gene Ther. Clin. Dev.* *25*, 72–84.
50. Meadows, A.S., Duncan, F.J., Camboni, M., Waligura, K., Montgomery, C., Zaraspe, K., Naughton, B.J., Bremer, W.G., Shilling, C., Walker, C.M., et al. (2015). A GLP-Compliant Toxicology and Biodistribution Study: Systemic Delivery of an rAAV9 Vector for the Treatment of Mucopolysaccharidosis IIIB. *Hum. Gene Ther. Clin. Dev.* *26*, 228–242.
51. Rosas, L.E., Grieves, J.L., Zaraspe, K., La Perle, K.M., Fu, H., and McCarty, D.M. (2012). Patterns of scAAV vector insertion associated with oncogenic events in a mouse model for genotoxicity. *Mol. Ther.* *20*, 2098–2110.
52. Wiseman, R.W., Karl, J.A., Bimber, B.N., O'Leary, C.E., Lank, S.M., Tuscher, J.J., Detmer, A.M., Bouffard, P., Levenkova, N., Turcotte, C.L., et al. (2009). Major histocompatibility complex genotyping with massively parallel pyrosequencing. *Nat. Med.* *15*, 1322–1326.
53. Wiseman, R.W., Karl, J.A., Bohn, P.S., Nimityongskul, F.A., Starrett, G.J., and O'Connor, D.H. (2013). Haplessly hoping: macaque major histocompatibility complex made easy. *ILAR J.* *54*, 196–210.
54. Xiao, X., Li, J., and Samulski, R.J. (1998). Production of high-titer recombinant adeno-associated virus vectors in the absence of helper adenovirus. *J. Virol.* *72*, 2224–2232.
55. Zolotukhin, S., Byrne, B.J., Mason, E., Zolotukhin, I., Potter, M., Chesnut, K., Summerford, C., Samulski, R.J., and Muzyczka, N. (1999). Recombinant adeno-associated virus purification using novel methods improves infectious titer and yield. *Gene Ther.* *6*, 973–985.